International Conference on Applied Energy 2020
Dec. 1 - Dec. 10, 2020, Bangkok / Virtual
Paper ID: 319

A nickel-based gradient porous electrode for efficient hydrogen evolution reaction

Yang Yang [1,2], Jun Li [1,2*], Yingrui Yang [1,2], Qian Fu [1,2], Liang Zhang [1,2], Qiang Liao [1,2], Xun Zhu [1,2]

1 Key Laboratory of Low-grade Energy Utilization Technologies and Systems, Chongqing University, Ministry of Education, Chongqing, 400044, China

2 Institute of Engineering Thermophysics, School of Energy and Power Engineering, Chongqing University, Chongqing, 400044, China

ABSTRACT

Great attention has been focused on the production of non-polluting gas fuel (hydrogen) from water electrolysis combined with renewable resources. However, the H_2 bubble removal during water electrolysis is still challenging, which is a critical factor to improve the electrode performance of hydrogen evolution reaction (HER). Herein, a gradient porous electrode with decreasing pore size from the middle of the electrode to the two sides (SML-LMS-HE) was developed to accelerate H_2 bubble removal rate by optimizing the pore size distribution of HER electrode. This electrode was prepared by using composite Ni foams with gradient porous structure as the conductive substrate, then being decorated with MoS_2/Ni_3S_2 heteronanorods. The as-prepared electrode exhibited a much higher H_2 bubble removal rate as compared with that of homogeneous porous HER electrode (MMM-MMM-HE) and gradient porous HER electrode with increasing pore size from the middle of the electrode to the two sides (LMS-SML-HE), conducive to the sufficient exposure of the active sites and the effective improvement of the electrode performance. As a result, SML-LMS-HE demonstrated a considerably low overpotential of 83 mV at the current density of 10 mA cm^{-2} as compared with MMM-MMM-HE and LMS-SML-HE.

Keywords: hydrogen evolution reaction, gradient porous electrode, hydrogen bubble transport, MoS_2/Ni_3S_2 heteronanorods

1. INTRODUCTION

In recent years, the massive consumption of fossil fuels has caused global resource depletion and environmental pollution. As a clean and sustainable energy, hydrogen is regarded as one of the best alternatives to fossil fuels [1]. For sustainable hydrogen production, the electrocatalytic hydrogen evolution reaction (HER) combined with renewable energy sources (e.g., solar energy and wind energy) is considered as one of the most promising pathways [2]. Currently, in order to reduce the overpotential and improve the efficiency of the HER, enormous HER electrodes have been developed by designing and synthesizing various eletrocatalysts on commercial conductive substrates, such as carbon paper, carbon cloth, titanium plate and Ni foam [3-6]. Although some eletrocatalysts have comparable HER performance with Pt-based eletrocatalysts considered as the most effective HER electrocatalysts [7], H_2 bubbles usually attach on the electrode surface during the HER process, covering the effective reaction area, increasing ohmic drop of electrolyzer, adding an additional mass transfer resistance for substrate and active species, thus deteriorating the HER performance [8]. Therefore, developing HER electrodes with efficient removal of H_2 bubbles to improve the HER performance remains an urgent problem to be solved.

It was reported that the structure optimization of electrode geometry was also an effective pathway to accelerate bubble transportation in electrochemical system [9-10]. Currently, Wang et al. proposed a new type of 3D nonwoven stainless steel fabric electrode for

Selection and peer-review under responsibility of the scientific committee of the 12th Int. Conf. on Applied Energy (ICAE2020).

electrocatalytic water splitting with a high gas bubble removal rate [9]. This electrode showed much higher current density under the same given overpotential as compared with the traditional Ni foam-based HER electrode. Therefore, developing new types of electrodes with optimized electrode geometry structure is a promising pathway to achieve rapid bubble removal rate, thus enhancing hydrogen evolution performance.

Herein, a new type of gradient porous electrode with decreasing pore size from the middle of the electrode to the two sides (SML-LMS-HE) and high H_2 bubble removal rate that can be produced by the hot press assembly of Ni foams (NFs) with different PPI was proposed. Then, porous MoS_2/Ni_3S_2 heteronanorods was loaded on SML-LMS-HE via solvothermal method. As a result, SML-LMS-HE demonstrated excellent HER performance, with a considerably low overpotential of 83 mV at the current density of 10 mA cm^{-2}, lower than that of MMM-MMM-HE (119 mV) and LMS-SML-HE (146 mV).

2. PAPER STRUCTURE EXPERIMENTAL SECTION

2.1 Fabrication of composite Ni foam conductive substrates (CNFs)

The gradient porous composite conductive substrates with decreasing pore size from the middle of the electrode to the both sides (SML-LMS-CNFs) were prepared by a stack-up pressing procedure. Firstly, six Ni foams (NFs) with different pore sizes stacked together, and from top to bottom were the NFs with 120, 50, 30, 30, 50 and 120 PPI, respectively. Then, using a hollow titanium with the thickness of 3 mm as a mold, a gradient porous precursor with the thickness of 3 mm was formed by pressing these six NFs at 2.3 MPa for 30 min. Finally, the gradient porous precursor was trimmed into a conductive substrate with the size of 25 × 10 × 3 mm3, named SML-LMS-CNF. For comparison, MMM-MMM-CNF and LMS-SML-CNF were prepared using the same procedure, except for the stacking order. The stacking order of MMM-MMM-CNF (a homogeneous porous composite conductive substrate) was NFs with 50, 50, 50, 50, 50 and 50 PPI from top to bottom, and the stacking order of LMS-SML-CNF (a gradient porous composite conductive substrate with increasing pore size from the middle of the electrode to the both sides) was NFs with 30, 50, 120, 120, 50 and 30 PPI from top to bottom. These three CNFs have the same mass of 620 ± 5 mg.

2.2 Loading MoS_2/Ni_3S_2 heteronanorods on Various

SML-LMS-HE was prepared by loading MoS_2/Ni_3S_2 on SML-LMS-CNF. In a typical process, a solution of 145.2 mg $NaMoO_4{\cdot}2H_2O$ and 456.8 mg CH_4N_2S was dissolved in 50 ml deionized water, and stirred for 30 min. Meanwhile, a SML-LMS-CNF was cleaned by sonication sequentially in 3 M hydrochloric acid, ethanol and deionized water for 15 min each. Then, the solution and the as-prepared SML-LMS-CNF were moved into a 100 ml Teflon-lined autoclave with steel shell. Thereafter, the autoclave was sealed and kept at 200℃ for 20 h, and naturally cooled to room temperature. Finally, the SML-LMS-HE was obtained by thoroughly cleaning with deionized water and ethanol and oven-dried. The MMM-MMM-HE and LMS-SML-HE were prepared, using the same process to load MoS_2/Ni_3S_2 on MMM-MMM-CNF and LMS-SML-CNF, respectively. The schematic for the entire preparation of SML-LMS-HE is shown in Fig. 1.

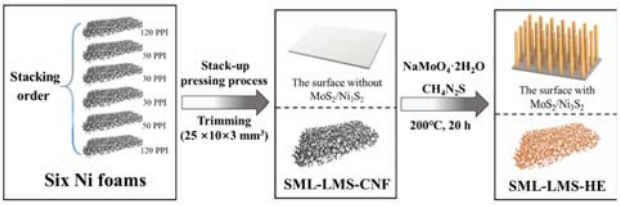

Fig 1 Scheme for the entire preparation of SML-LMS-HE

2.3 Physical and Chemical Characterization

State the objectives of the work and provide an adequate background, avoiding a detailed literature survey or a summary of the results. The pore size distributions of three HER electrodes and the morphologies of MoS_2/Ni_3S_2 heteronanorods were performed by scanning electron microscope and high-resolution transmission electron microscopy (SEM: Hitachi SU8020, HRTEM: Tecnai G2 F20). The chemical compositions of MoS_2/Ni_3S_2 heteronanorods were characterized by X-ray diffraction and X-ray photoelectron spectroscopy (XRD: D8 ADVANCE, XPS: Thermo ESCALAB 250Xi). Energy-dispersive X-ray spectroscopy (EDX) and elemental mapping of Mo, Ni and S on the electrodes were conducted by the same instruments as HRTEM. The S elemental of three HER electrodes was analyzed by inductively coupled plasma mass spectrometry (ICP-MS: Agilent 7700). The images of the removal process of H_2 bubbles were recorded using a Pointgray GS3-U3 charge-coupled device (CCD) camera equipped with a Navitar lens. A LED plane light source system provided the illumination.

3. RESULT AND DISCUSSION

3.1 *Physicochemical Characterization*

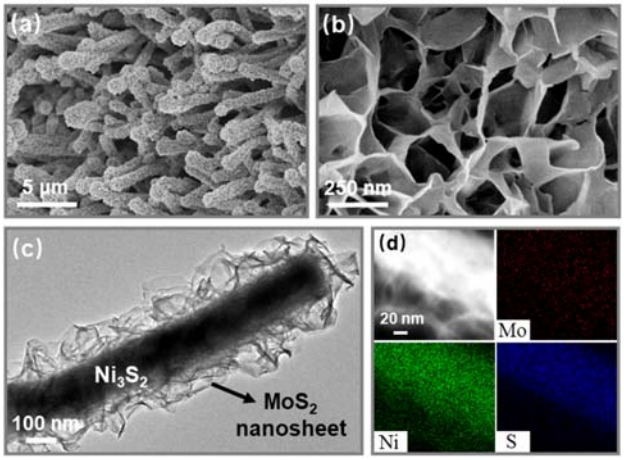

Fig 2 (a-b) Catalyst morphologies at different magnifications. (c) High-resolution TEM images and (d) its elemental maps

The MoS_2/Ni_3S_2 architectures on SML-LMS-HE were observed by SEM. As shown in Fig. 2a-b, The porous MoS_2/Ni_3S_2 heteronanorods arrays were evenly attached on the surface of the SML-LMS-HE, and the pore diameters of the porous MoS_2/Ni_3S_2 heteronanorods were 15 - 140 nm. The porous nanostructures greatly increased the ECSA of the HER electrode due to a high specific surface area. In addition, since the pores of electrocatalysts are mainly mesopores and macropores, thereby enhancing the transfer of substrate and active species. In conclusion, MoS_2/Ni_3S_2 heteronanorods on SML-LMS-HE were beneficial to the improvement of HER performance of electrode. The microstructure of these heteronanorods was further performed by TEM (Fig. 2c). The diameter of the porous MoS_2/Ni_3S_2 heteronanorods is about 360 nm. Furthermore, the elemental mapping showed the uniform distribution of Ni, Mo and S in MoS_2/Ni_3S_2 heteronanorods (Fig. 2d). The above results indicated a hierarchical porous structure with macro (Ni foams, macro pores at μm size) and nano (MoS_2/Ni_3S_2 heteronanorods, nano pores at nm size) was successfully formed on the surface of electrodes.

3.2 Bubble Behaviors

To compare the bubble behavior of three HER electrodes, a visualization experiment was carried out on SML-LMS-HE, MMM-MMM-HE and LMS-SML-HE at -30 mA cm^{-2}. As shown in Fig. 3a-d, the H_2 bubbles quickly escaped from the SML-LMS-HE electrode within 1.87 s. As a comparison, MMM-MMM-HE and LMS-SML-HE showed a much slower H_2 bubble removal process during the HER. Accompanied with the nucleation, growth and detachment, it took 4.20 s to release H_2 bubbles from the MMM-MMM-HE electrode (Fig. 3e-h). As shown in Fig. 3i-l, LMS-SML-HE spent 6.20 s releasing H_2 bubble from electrode. The high H_2 bubble removal rate from SML-LMS-HE electrode was ascribed to its large pore size inside electrode, which decreased the resistance slowing down H_2 bubbles escaping rate, thus avoiding H_2 bubbles getting trapped into pore channels. Furthermore, the small pore size of SML-LMS-HE distributed in both sides of electrode could induce a stronger Marangoni convection outside the electrode, which accelerated the removal rate of bubbles, resulting from a higher specific surface area of the small pore layer resulting from a large specific surface of small pore layers [11-13].

s

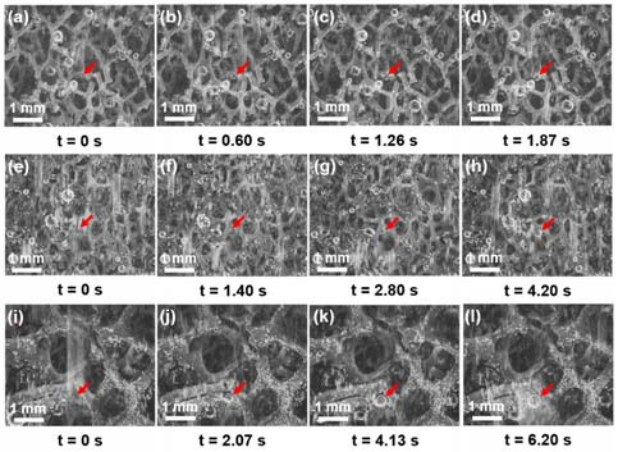

Fig 3 Digital photos demonstrating the bubble removal process on (a-d) SML-LMS-HE, (e-h) MMM-MMM-HE and (i-l) LMS-SML-HE. Red arrow indicates the evolution process of a typical hydrogen bubble.

3.3 *Electrocatalytic Performance*

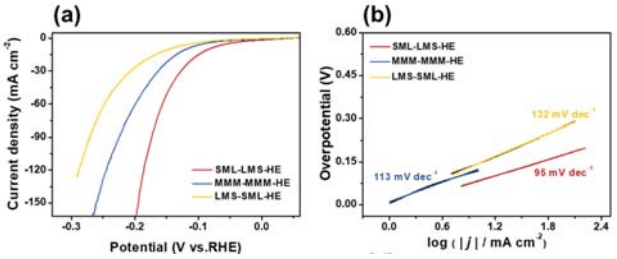

Fig 4 (a) LSV curvres and (b) Tafel plots for SML-LMS-HE, MMM-MMM-HE and LMS-SML-HE. (c) Stability of SML-LMS-HE at -10 mA cm^{-2} for 18 h, and (d) LSV curve before and after test.

The HER performance of SML-LMS-HE, MMM-MMM-HE and LMS-SML-HE was conducted with a three-electrode system. Fig. 4a showed the HER activities of three HER electrodes, followed the order of SML-LMS-HE > MMM-MMM-HE > LMS-SML-HE. The optimized SML-LMS-HE exhibited excellent HER electrocatalytic activity with a low overpotential of 83 mV at a current density of

10 mA cm^{-2}, whereas the MMM-MMM-HE and the SML-LMS-HE required about 119 and 146 mV of overpotential to reach the same current density. What's more, a further increase of current densities led to a slow rise in overpotential of SML-LMS-HE (an overpotential of 177 mV reach 100 mA cm^{-2}). The excellent HER performance of SML-LMS-HE was owing to the optimized porous structure, which accelerated the removal of H_2 bubble, thereby increasing the number of effective active sites. Additionally, Fig. 4b showed that the Tafel slop of SML-LMS-HE was the lowest (95 mV dec^{-1}) as compared with the other two HER electrodes (113 mV dec^{-1} for MMM-MMM-HE, 132 mV dec^{-1} for LMS-SML-HE, respectively). The low Tafel slop indicated a faster increase of the HER rate with increasing overpotential. This result confirmed again that a high H_2 bubble removal rate can greatly improve the HER performance of SML-LMS-HE, due to the optimized porous structure.

4. CONCLUSIONS

In conclusion, we have developed a new type of gradient porous electrode (SML-LMS-HE). It was found that the as-prepared SML-LMS-HE electrode showed a high H_2 bubble removal rate as compared with MMM-MMM-HE (a homogeneous porous HER electrode) and LMS-SML-HE (another gradient porous electrode) during the HER, which attributes to that the large pore size inside electrode could accelerate H_2 bubble escaping from pore channels, and the small pore size outside electrode could lead to a stronger Marangoni convection, further accelerating the detachment of bubble. This study provides an alternative strategy to improve HER performance by accelerating bubble removal rate from HER electrodes and will inspire further efforts to develop the electrodes with optimized structure for not only hydrogen evolution but also other key technologies of energy conversion and storage.

ACKNOWLEDGEMENT

This work was supported by the National Natural Science Funds for Outstanding Young Scholar (No. 51622602), Program for Back-up Talent Development of Chongqing University (No. cqu2018CDHB1A03), National Science Foundation for Young Scientists of China (No. 51506017), National Science Foundation for Young Scientists of China (No. 51606022), and Natural Science Foundation of Chongqing (No. cstc2015jcyjA90017).

REFERENCE

[1] Dresselhaus MS, Thomas IL. Alternative energy technologies[J]. Nature, 2001, 414(6861):332.

[2] Ngoh S K, Njomo D. An overview of hydrogen gas production from solar energy[J]. Renewable & Sustainable Energy Reviews, 2012, 16(9):6782-6792.

[3] Xue Y, Hui L, Yu H, et al. Rationally engineered active sites for efficient and durable hydrogen generation[J]. Nature communications, 2019, 10(1): 2281.

[4] Dang Q, Sun Y, Wang X, et al. Carbon dots-Pt modified polyaniline nanosheet grown on carbon cloth as stable and high-efficient electrocatalyst for hydrogen evolution in pH-universal electrolyte[J]. Applied Catalysis B: Environmental, 2019, 257: 117905.

[5] Zhai L, Mak C H, Qian J, et al. Self-reconstruction mechanism in NiSe2 nanoparticles/carbon fiber paper bifunctional electrocatalysts for water splitting[J]. Electrochimica Acta, 2019, 305: 37-46.

[6] Chen Y, Ren Z, Fu H, et al. NiSe-Ni0.85Se Heterostructure Nanoflake Arrays on Carbon Paper as Efficient Electrocatalysts for Overall Water Splitting[J]. Small, 2018, 14(25): 1800763.

[7] Chen C, Kang Y, Huo Z, et al. Highly crystalline multimetallic nanoframes with three-dimensional electrocatalytic surfaces[J]. Science, 2014, 343(6177): 1339-1343.

[8] Zeng K, Zhang D. Recent progress in alkaline water electrolysis for hydrogen production and applications[J]. Progress in energy and combustion science, 2010, 36(3): 307-326.

[9] Wang L, Huang X, Jiang S, et al. Increasing Gas Bubble Escape Rate for Water Splitting with Nonwoven Stainless Steel Fabrics[J]. ACS applied materials & interfaces, 2017, 9(46): 40281-40289.

[10] Taqieddin A, Nazari R, Rajic L, et al. Physicochemical hydrodynamics of gas bubbles in two phase electrochemical systems[J]. Journal of The Electrochemical Society, 2017, 164(13): E448-E459.

[11] Massing J, Mutschke G, Baczyzmalski D, et al. Thermocapillary convection during hydrogen evolution at microelectrodes[J]. Electrochimica Acta, 2019, 297: 929-940.

[12] Yang X, Baczyzmalski D, Cierpka C, et al. Marangoni convection at electrogenerated hydrogen bubbles[J]. Physical Chemistry Chemical Physics, 2018, 20(17): 11542-11548.

[13] Zhao X, Ren H, Luo L. Gas bubbles in electrochemical gas evolution reactions[J]. Langmuir, 2019, 35(16): 5392-5408.